Support Information

Boosting the activity and stability via Co nanoparticles and MoC synergistic catalysis to construct a bifunctional electrocatalyst for high-performance and long-life rechargeable zinc-air batteries

Xiaohua Deng[a], Xianrui Gu[b], Yingjie Deng[a], Zhu Jiang[a], Wenxuan Chen [a], Dai Dang[a,*], Wei Lin[b,*], Bin Chi [a,*]

[a] School of Chemical Engineering and Light Industry, Guangdong University of Technology, Guangzhou, Guangdong, 510006, P. R. China.

[b] Research Institute of Petroleum Processing, Sinopec, No. 18, Xueyuan Road, Haidian District, Beijing 100083, China.

∗ Corresponding author.

E-mail address: dangdai@gdut.edu.cn (d. Dang)

1. Characterization

The morphologies and structures of the catalysts were recorded with scanning electron microscopy (SEM, SU8220 Hitachi High-Tech). Transmission electron microscope (TEM) was conducted on a JEOL JEM2100 TEM with a field emission gun operating at 200 kV. EDS analysis was performed on an AMETEK Materials Analysis EDX equipped on the TEM. The phase characteristics of samples are measured on X-ray diffraction (XRD, Dandong Tongda Science & Technology) with a Cu Kα radiation (λ = 1.5406 Å). Raman spectra were performed on UV Laser Raman Spectroscopy (HORIBA) with an excitation wavelength of 633 nm. Specific surface areas were calculated by the Brunaure–Emmert–Teller method. Brunauer–Emmett–Teller (BET) specific surface area and pore size distribution measurement employed a Tristar 3020 gas adsorption analyzer at 77 K. Pore volumes and sizes were estimated from the pore-size distribution curves from the adsorption isotherms using the Barrett–Joyner–Halenda method. X-ray photoelectron spectroscopy (XPS) was conducted with an AXIS Supra by Kratos Analytical Inc. (using monochromatized Al Kα radiation (HV = 1486.6 eV, 225 W) as an X-ray source with a base pressure of 10−9 torr, A charge neutralizer was used throughout as the samples were mounted such that they were electrically isolated from the sample bar. All spectrums were calibrated by C 1s (284.8 eV).

2. Electrochemical measurement

All electrochemical tests were performed on the Ivium Station workstation at room temperature. A three-electrode system evaluated all ORR and OER performance tests. The working electrode was a rotating disk electrode (RDE) with a diameter of 5 mm (0.196 cm^2) or a rotating ring disk electrode (RRDE) with a diameter of 5.61 mm (0.247 cm^2). The counter electrode was a graphite rod. The reference electrode was a saturated Ag/AgCl electrode in the acidic medium and a saturated Hg/HgO electrode in the alkaline medium. The cyclic voltammetry (CV) test was carried out in 0.1 M KOH or 0.5 M H_2SO_4 filled with N_2 or O_2 (scan rate is 50 $mV \cdot s^{-1}$). The linear sweep voltammetry (LSV) test was carried out in 0.1 M KOH or 0.5 M H_2SO_4 filled with O_2

at a speed range of 1600 rpm (scan rate is 5 $mV \cdot s^{-1}$). Current time Chrono current response was measured at 0.66 V (relative to RHE) in the alkaline medium and 0.45 V (relative to RHE) in the acidic medium. The final oxygen reduction currents were obtained by subtracting the background currents measured in the N_2-purged electrolyte from those measured in the O_2-saturated electrolyte. Current time Chrono current response was estimated at 0.66 V (relative to RHE) in the alkaline medium and 0.45V(relative to RHE) in the acidic medium. In the OER test, the working electrode is a glassy carbon (GC) electrode with a diameter of 3 mm (0.07 cm^2). The counter electrode is a graphite rod, and the reference electrode is a saturated Hg/HgO electrode. The LSV test is tested in 1 M KOH (scan rate of 5 $mV \cdot s^{-1}$).

The catalyst used for the ORR and OER test was prepared as follows: 5 mg of the catalyst was dispersed in a 1 mL mixed solution containing ethanol and Nafion solution (5 wt%). The mixed solution was sonicated for 1 h to form a uniform suspension. Then, take out 20 μL of the catalyst solution from the pipette and drop it evenly on the rotating disk (RDE) electrode. After natural drying, a uniform film is formed. The catalyst load is approximately 500 μg cm^{-2}.

RRDE tests were taken to measure the peroxide (H_2O_2) yield and the electron transfer number (n) using the following equations:

$$H_2O_2\% = \frac{i_R/N_0}{i_R + i_R/N_0} \times 200\%$$

$$n = 4 \times \frac{i_D}{i_D + {i_R}/{N_0}}$$

I_D is the disk current, i_R is the ring current, and current collection efficiency (0.37) of RRDE.

OER measurement: Calculate the potential corresponding to the reversible hydrogen electrode (RHE) electrode by the following formula:

$$E_{(RHE)} = E_{Hg/HgO} + (0.098 + 0.0591 \times PH)$$

The following formula calculates the overpotential (η):

$$\eta = E_{RHE} - 1.23$$

3. Zn-air battery performance test

All ZAB tests were performed at room temperature on the Ivium Station workstation. Each charge and discharge cycle were 20 minutes, and the current density was 5 mA cm^{-2}. LSV was recorded to record the charge and discharge polarization curve, and the scan rate was fixed at 10 mV s^{-1}. The discharge characteristic curve was obtained by testing at a current density of 20 mA cm^{-2}. Both current density and power density were normalized to the effective surface area of the air electrode.

Battery-specific energy calculation formula:

$$specific\ capacity = \frac{current \times service\ hour}{weight\ of\ consumed\ zinc}$$

Energy density calculation formula:

$$energy\ density = \frac{current \times service\ hour \times arrage\ discharge\ voltage}{weight\ of\ consumed\ zinc}$$

By varying the current density (from 1 mA cm^{-2} to 20 mA cm^{-2}) for a constant current discharge test, the discharge stability of the ZAB can be observed. Then, the discharge multiplier performance and reversibility of the ZAB were determined by adjusting the current density from 20 mA cm^{-2} to 1 mA cm^{-2}.

Preparation of the air cathode: A carbon cloth (2×2 cm^2) was attached to the gas diffusion layer (2×2 cm^2) by hot pressing. 4 mg of the catalyst was dissolved in 1 mL of ethanol, then dropped into 11 μL of PTFE solution (6 wt%), and sonicated for 30 minutes to form a uniform suspension. Spread the catalyst suspension uniformly on the side of the carbon paper without the microporous layer, with a loading of approximately 1 mg cm^{-2}. After the catalyst solvent evaporates, the obtained electrode can be prepared for Zn-air battery assembly and further testing.

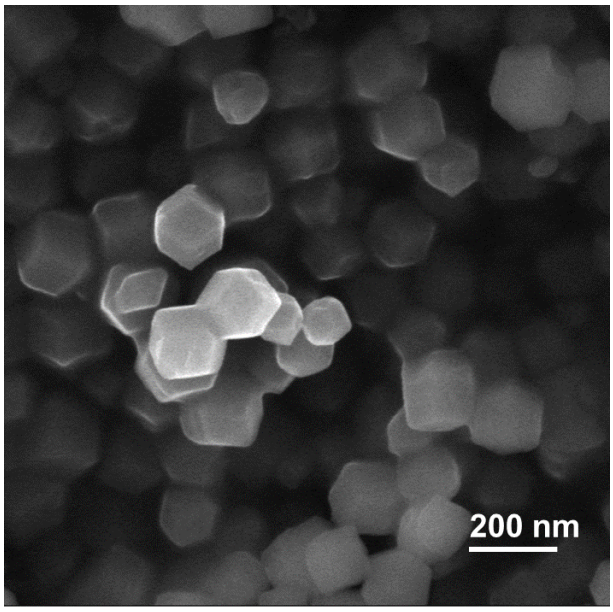

Fig. S1 The SEM image of the precursor ZIF-CoZn

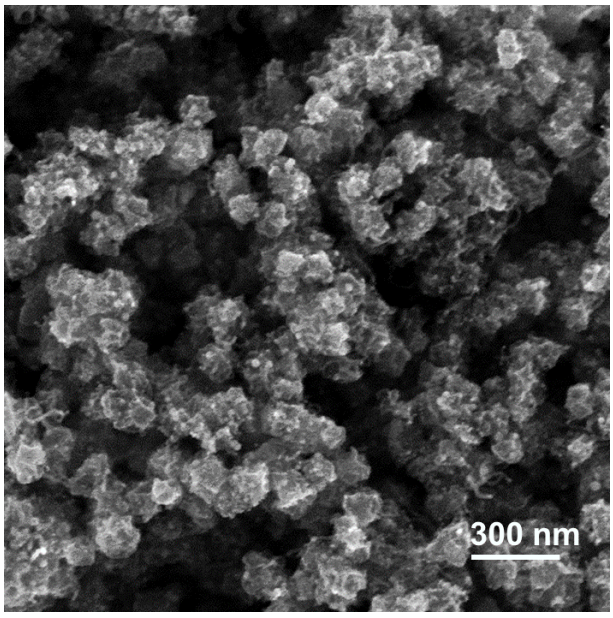

Fig. S2 The SEM image of the Co-NC

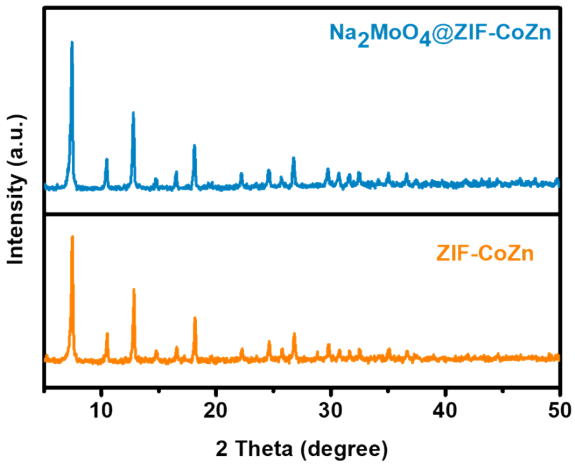

Fig. S3 The XRD image of ZIF-CoZn and Na_2MoO_4@ ZIF-CoZn

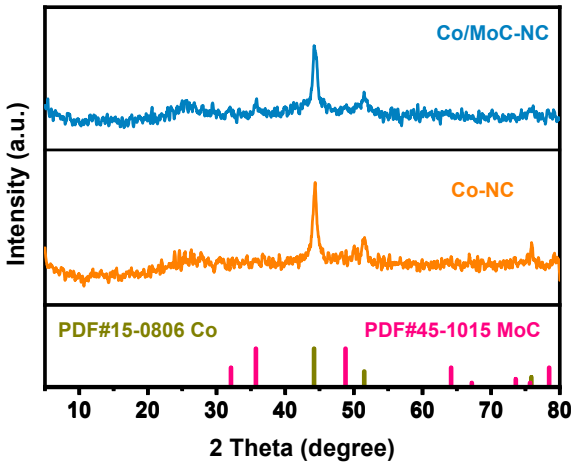

Fig. S4 The XRD image of Co/MoC-NC and Co-NC

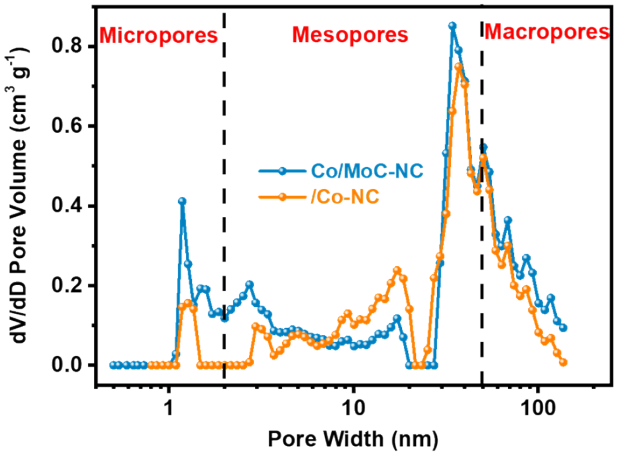

Fig. S5 The pore size distribution patent of Co/MoC-NC and Co-NC

Table S1 Surface areas, mesopore volumes, and mesoporosity of Co-NC and Co/MoC-NC

Sample	S_{BET} ($m^2 \cdot g^{-1}$)	V_{mes} ($cm^3 \cdot g^{-1}$)	Mesoporosity (%)
Co-NC	248.21	0.7039	63.21
Co/MoC-NC	395.06	0.8509	65.75

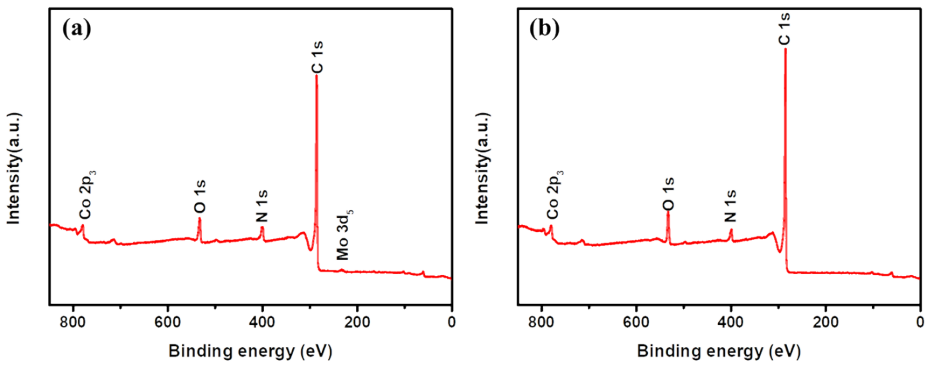

Fig. S6 The XPS spectrum of (a) Co/MoC-NC and (b) Co-NC

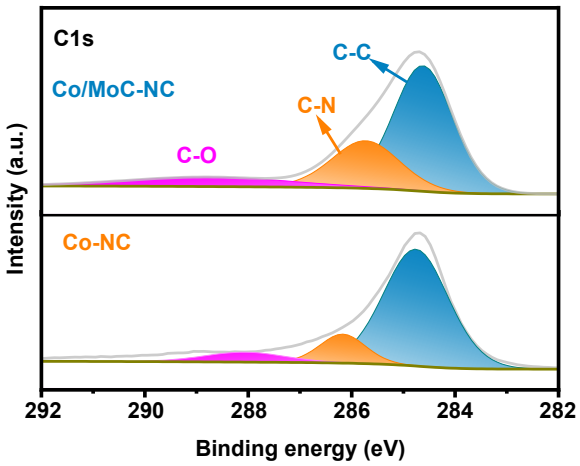

Fig. S7 High-resolution C1s XPS spectra of Co/MoC-NC and Co-NC

Table S2 Fraction of the different Co species present in Co-NC and Co/MoC-NC

Sample	Co(0) (at %)	Co^{3+} (at%)	Co^{2+} (at%)	Sat. (at%)
Co-NC	19.85	32.60	36.36	11.19
Co/MoC-NC	30.94	32.30	25.37	11.39

Table S3 Fraction of the different Mo species present in Co/MoC-NC

Sample	Mo^{6+} (at %)	Mo^{4+} (at%)	Mo^{2+} (at%)
Co/MoC-NC	19.93	43.96	36.11

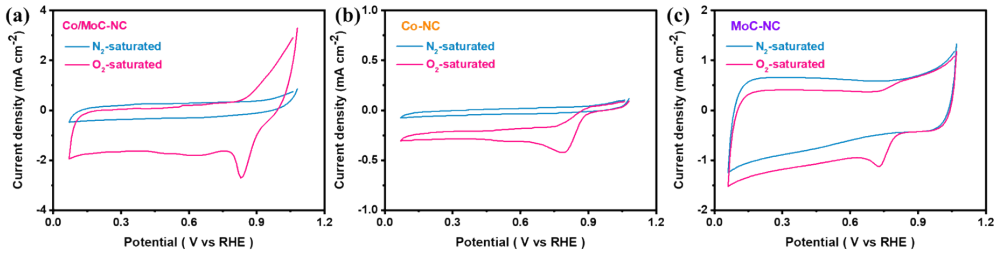

Fig. S8 In 0.1M KOH, CV curves of (a) Co/MoC-NC, (b) Co-NC, and (c) MoC-NC under O_2 and N_2 saturated conditions

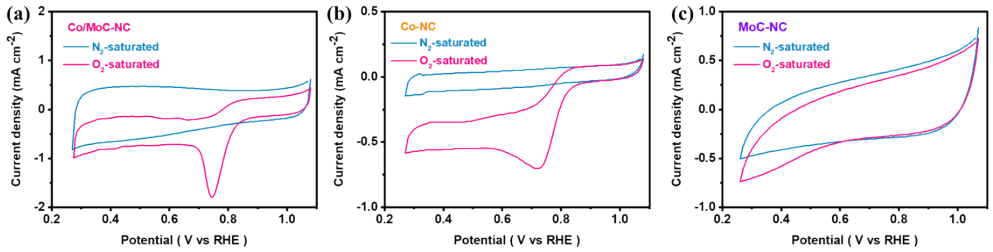

Figure S9 In 0.5M H_2SO_4, CV curves of (a) Co/MoC-NC, (b) Co-NC, and (c) MoC-NC under O_2 and N_2 saturated conditions

Table S4 ORR performance comparison of various catalysts in alkaline electrolytes

Catalyst	**$E_{1/2}$ (mV vs RHE)**	**j(mA cm^{-2})**	**Reference**
Co/Mo-NC	0.87	6.5	This work
Co/NC	0.83	4.5	[1]
Co/HNCP	0.84	5.4	[2]
Co 3 mmol N/C	0.84	6.0	[3]
Co@NCNRs	0.84	5.5	[4]

Co-SAs@N-CNS	0.84	4.7	[5]
Co-N-C	0.80	4.5	[6]
Co/CoO/NG-900	0.80	4.5	[7]
Co/N,S-CN-900	0.74	4.2	[8]
Co-NC-AD	0.86	6.2	[9]
Co/NHPC-800	0.82	6.4	[10]

Table S5 OER performance comparison of various catalysts in alkaline electrolytes

Catalyst	**η_{10} (mV@10 mA cm^{-2})**	**Electrolyte**	**Reference**
Co/Mo-NC	320	1 M KOH	This work
MoS_2/Co-N-CN_2	400	1 M KOH	[11]
Co_2P	364	1 M KOH	[12]
CoMnNiS	371	1 M KOH	[13]
Co@NrC-0.3	386	1 M KOH	[14]
P-CoNi@NSCs	350	0.1 M KOH	[15]
Co-N/C	330	1 M KOH	[16]
Co@N-PCNF-1	440	0.1 M KOH	[17]
Co/N–CNF	380	1 M KOH	[18]
Co2P/doped-CNTs-1000	343	1 M KOH	[19]
Co-Ni (trace)/NCNTs	337	1 M KOH	[20]

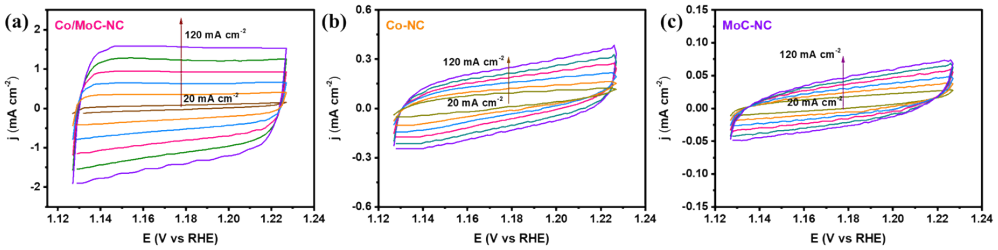

Figure S10 CV curves of the (a) Co/MoC-NC, (b) Co-NC, and (c) MoC-NC at various scan rates.

Table S6 Comparison of the ZABs performance

Catalyst	Open circuit voltage(V)	Power density (mW cm^{-2})	Reference
Co/MoC-NC	1.51	214.5	This work
Fe/Co/Zn-CNZIF	1.46	156.7	[21]
Co@CNT-NC	1.52	179.3	[22]
FeZn4Co@CNFs	1.496	107.6	[23]
CoFe-NCNFs	1.522	156.3	[24]
Co@NCNRs	1.54	76.76	[4]
Co/N-CNSNs	1.47	81.7	[25]
Co-N-C	1.54	132	[26]
Co/NHPC-800	1.5	40	[27]
Co/Co-N-C	1.434	122.5	[28]
Co-NDC	1.3	154	[29]
Co/CoO@NSC	1.53	187.6	[29]
Co-Ni-S@NSPC	1.539	100	[30]
Co@N-C700	1.41	133	[31]

CNT@SAC-Co/NCP	1.45	172	[32]
Co@hNCTs-800	1.45	149	[33]

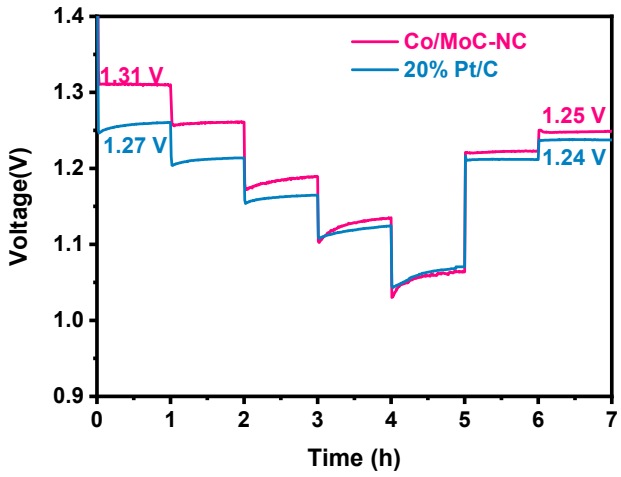

Fig. S11 Multiplier performance testing of the Zn-air batteries assembled with Co/MoC-NC and 20% Pt/C

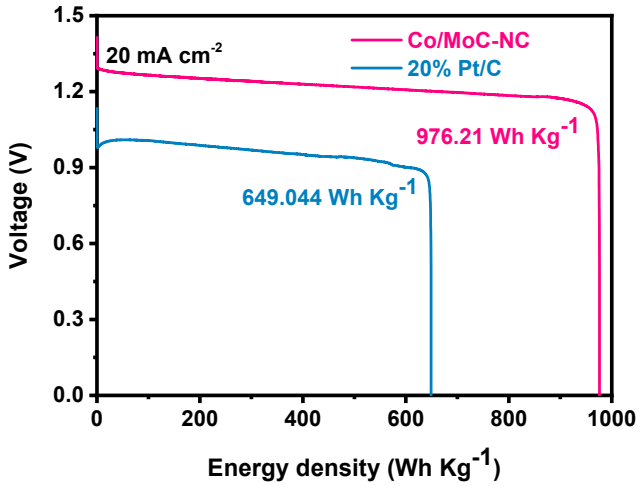

Fig. S12 Energy density of the Zn-air batteries assembled with Co/MoC-NC and 20% Pt/C

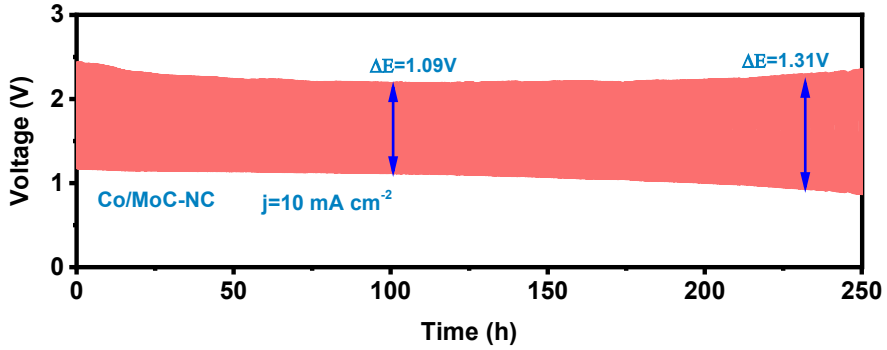

Fig. S13 Discharge-charge cycling curves of the batteries assembled by Co/MoC-NC at 10 mA cm^{-2} (20 min per cycle).

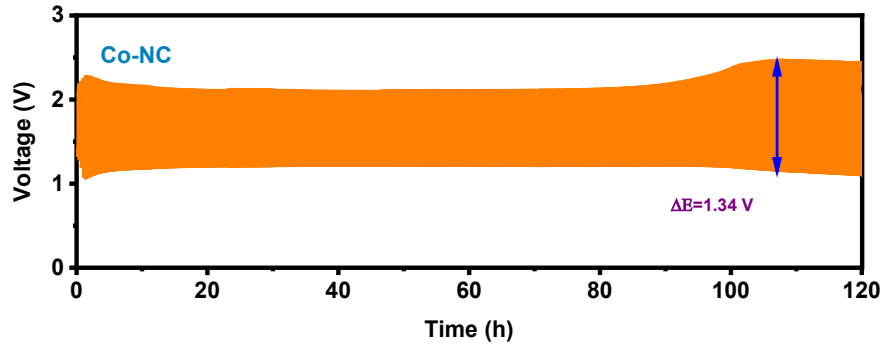

Fig. S14 Discharge-charge cycling curves of the batteries assembled by Co-NC at 5 mA cm^{-2} (20 min per cycle).

Table S7 Comparison of the ability of ZABs assembled with different catalysts

Catalyst	Density current (mA cm^{-2})	Hour(h)	Reference
Co/MoC-NC	5	300	This work
Co/MoC-NC	10	250	This work
CoNi-CoO-NiO@NC-800	2	78	[34]

Mn-CoNx/N-PC	5	35	[35]
Co-N-C	5	50	[36]
Co@N-C/PCNF	5	90	[37]
FeCo/NG	5	100	[38]
Co@bCNTs	5	110	[39]
Co_9S_8/CoNSC	10	40	[40]
Co/N–CNFs	10	50	[41]
CuCoSe@NC-2	10	130	[42]
Co/N–CNTs-2	10	200	[43]

Reference

[1] A. Aijaz, J. Masa, C. Rosler, W. Xia, P. Weide, A.J.R. Botz, R.A. Fischer, W. Schuhmann, M. Muhler, Co@Co3O4 Encapsulated in Carbon Nanotube-Grafted Nitrogen-Doped Carbon Polyhedra as an Advanced Bifunctional Oxygen Electrode, Angew Chem Int Edit, 55 (2016) 4087-4091.

[2] D.N. Ding, K. Shen, X.D. Chen, H.R. Chen, J.Y. Chen, T. Fan, R.F. Wu, Y.W. Li, Multi-Level Architecture Optimization of MOF-Templated Co-Based Nanoparticles Embedded in Hollow N-Doped Carbon Polyhedra for Efficient OER and ORR, Acs Catal, 8 (2018) 7879-7888.

[3] K. Seonghee, J. Seulgi, Y. Hyunsoo, S. Hyunji, C. Heechae, K. Jun, L.L. Oi, Near surface electric field enhancement: Pyridinic-N rich few-layer graphene encapsulating cobalt catalysts as highly active and stable bifunctional ORR/OER catalyst for seawater batteries, Applied Catalysis B: Environmental, (2022).

[4] Y. Qiang, L. Jianshuai, L. Jiantao, Y. Ruohan, W. Jinsong, X. Shibo, L. Xinyuan, X. Nuo, Z. Liang, M. Liqiang, ZIF-mediated anchoring of Co species on N-doped carbon nanorods as an efficient cathode catalyst for Zn-air batteries, Energy Environ Mater, (2022).

[5] L.B. Zong, K.C. Fan, W.C. Wu, L.X. Cui, L.L. Zhang, B. Johannessen, D.C. Qi, H.J. Yin, Y. Wang, P.R. Liu, L. Wang, H.J. Zhao, Anchoring Single Copper Atoms to Microporous Carbon Spheres as High-Performance Electrocatalyst for Oxygen Reduction Reaction, Adv Funct Mater, 31 (2021).

[6] M.R. Liu, H. Lin, Z.W. Mei, J.L. Yang, J. Lin, Y.D. Liu, F. Pan, Tuning Cobalt and Nitrogen Co-Doped Carbon to Maximize Catalytic Sites on a Superabsorbent Resin for Efficient Oxygen Reduction, Chemsuschem, 11 (2018) 3631-3639.

[7] W. Jing, Z. Haihong, E.-W. Luis Alberto, L. Huiyu, A.-V. Nicolas, L. Danqing, T. Pinggui, F. Yongjun, Synthesis and electrocatalytic performance of N-doped graphene embedded with Co/CoO nanoparticles towards oxygen evolution and reduction reactions, Catal Commun, (2022).

[8] S. Rui-Min, R. Qi-Dong, F. Jiu-Ju, Z. Lu, W. Ai-Jun, Sandwich-like superstructure of in-situ self-assembled hetero-structured carbon nanocomposite for improving

electrocatalytic oxygen reduction, J Colloid Interf Sci, (2022).
[9] F. Yu, S. Kexin, Z. Wei, Z. Xinyan, Y. Seung Jo, K. Jin-Gyu, Q. Sifan, Q. Yugang, Z. Xu, C. Zhongjun, Q. Tingting, Y. Nailin, W. Zizhun, L. Dabing, Z. Weitao, Efficient ORR catalysts for zinc-air battery: Biomass-derived ultra-stable Co nanoparticles wrapped with graphitic layers via optimizing electron transfer, J Energy Chem, (2022).
[10] Z. Wenshu, L. Yanyan, L. Huan, W. Dichao, Z. Gaoyue, J. Jianchun, Co/N-Doped hierarchical porous carbon as an efficient oxygen electrocatalyst for rechargeable Zn–air battery, Rsc Adv, (2021).
[11] X.B. Hou, H.M. Zhou, M. Zhao, Y.B. Cai, Q.F. Wei, MoS2 Nanoplates Embedded in Co-N-Doped Carbon Nanocages as Efficient Catalyst for HER and OER, Acs Sustain Chem Eng, 8 (2020) 5724-5733.
[12] B.T. Jebaslinhepzybai, T. Partheeban, D.S. Gavali, R. Thapa, M. Sasidharan, One-pot solvothermal synthesis of Co2P nanoparticles: An efficient HER and OER electrocatalysts, Int J Hydrogen Energ, 46 (2021) 21924-21938.
[13] M. Verma, L. Sinha, P.M. Shirage, Electrodeposited nanostructured flakes of cobalt, manganese and nickel-based sulfide (CoMnNiS) for electrocatalytic alkaline oxygen evolution reaction (OER), J Mater Sci-Mater El, 32 (2021) 12292-12307.
[14] J. Yu, Y.W. Dai, Z.B. Zhang, T. Liu, S.Y. Zhao, C. Cheng, P. Tan, Z.P. Shao, M. Ni, Tailoring structural properties of carbon via implanting optimal co nanoparticles in n-rich carbon cages toward high-efficiency oxygen electrocatalysis for rechargeable zn-air batteries, Carbon Energy, (2022).
[15] H. Xianhong, F. Jing, N. Mengyuan, L. Pengfei, Z. Qing, B. Zhengyu, Y. Lin, Long-range interconnected nanoporous Co/Ni/C composites as bifunctional electrocatalysts for long-life rechargeable zinc-air batteries, Electrochim Acta, (2022).
[16] W. Zhang, C.H. Xu, H. Zheng, R. Li, K. Zhou, Oxygen-Rich Cobalt-Nitrogen-Carbon Porous Nanosheets for Bifunctional Oxygen Electrocatalysis, Adv Funct Mater, (2022).
[17] W. Mingxing, T. Xiyao, Y. Wenlu, G. Bingran, G. Jianing, Co nanoparticles embedded in wheat-like porous carbon nanofibers as bifunctional electrocatalysts for rechargeable zinc-air batteries, Electrochim Acta, (2022).

[18] L. Jin, Z. Jinsong, K.H.L. Michael, Valence Engineering of Polyvalent Cobalt Encapsulated in a Carbon Nanofiber as an Efficient Trifunctional Electrocatalyst for the Zn–Air Battery and Overall Water Splitting, Acs Appl Mater Inter, (2022).

[19] S. Li, F. Haiyun, F. Xiaoli, G. Hao, W. Tao, H. Jianping, A simultaneous phosphorization and carbonization strategy to synthesize a defective Co2P/doped-CNTs composite for bifunctional oxygen electrocatalysis, Chem Eng J, (2022).

[20] Y.D. Shi, J.N. Cai, X.F. Zhang, Z.S. Li, S. Lin, Promotional effects of trace Ni on its dual-functional electrocatalysis of Co/N-doped carbon nanotube catalysts for ORR and OER, Int J Hydrogen Energ, 47 (2022) 7761-7769.

[21] G. Zanwu, M. Yanan, Z. Yueju, S. Yi, T. Shaoru, W. Qian, L. Wei, Trimetallic ZIFs-derived porous carbon as bifunctional electrocatalyst for rechargeable Zn-air battery, J Power Sources, (2022).

[22] G. Bifen, T. Mingyue, X. Wenhao, L. Xiufang, L. Zongnan, S. Manrong, L. Bizhou, Co-embedded carbon nanotubes modified N-doped carbon derived from poly(Schiff base) and zeolitic imidazole frameworks as efficient oxygen electrocatalyst towards rechargeable Zn-air battery, J Power Sources, (2022).

[23] W. Fuling, X. Zuoxu, L. Xue, R. Jianwei, X. Tao, L. Zhi, L. Xiyou, C. Yanli, Strategic design of cellulose nanofibers@zeolitic imidazolate frameworks derived mesoporous carbon-supported nanoscale CoFe2O4/CoFe hybrid composition as trifunctional electrocatalyst for Zn-air battery and self-powered overall water-splitting, J Power Sources, (2021).

[24] L. Shi-Yi, C. Yu-Ping, C. Ying, Z. Lu, F. Jiu-Ju, W. Ai-Jun, Aminouracil-assisted synthesis of CoFe decorated bougainvillea-like N-doped carbon nanoflowers for boosting Zn–air battery and water electrolysis, J Power Sources, (2021).

[25] X.X. Huang, Y.L. Zhang, H.M. Shen, W. Li, T. Shen, Z. Ali, T. Tang, S.J. Guo, Q. Sun, Y.L. Hou, N-Doped Carbon Nanosheet Networks with Favorable Active Sites Triggered by Metal Nanoparticles as Bifunctional Oxygen Electrocatalysts, Acs Energy Lett, 3 (2018) 2914-2920.

[26] Y. Peng, W. Lei, S. Fanfei, X. Ying, L. Xu, M. Jingyuan, W. Xiuwen, T. Chungui, L. Jinghong, F. Honggang, Co Nanoislands Rooted on Co–N–C Nanosheets as Efficient

Oxygen Electrocatalyst for Zn–Air Batteries, Adv Mater, (2019).
[27] P. Yu, L. Wang, F.F. Sun, Y. Xie, X. Liu, J.Y. Ma, X.W. Wang, C.G. Tian, J.H. Li, H.G. Fu, Co Nanoislands Rooted on Co-N-C Nanosheets as Efficient Oxygen Electrocatalyst for Zn-Air Batteries, Adv Mater, 31 (2019).
[28] D. Wang, P.X. Yang, H. Xu, J.Y. Ma, L. Du, G.X. Zhang, R.P. Li, Z. Jiang, Y. Li, J.Q. Zhang, M.Z. An, The dual-nitrogen-source strategy to modulate a bifunctional hybrid Co/Co-N-C catalyst in the reversible air cathode for Zn-air batteries, J Power Sources, 485 (2021).
[29] Z.Y. Chen, Q.C. Wang, X.B. Zhang, Y.P. Lei, W. Hu, Y. Luo, Y.B. Wang, N-doped defective carbon with trace Co for efficient rechargeable liquid electrolyte-/all-solid-state Zn-air batteries, Sci Bull, 63 (2018) 548-555.
[30] D. Zhou, H.Q. Fu, J.L. Long, K. Shen, X.L. Gou, Novel fusiform core-shell-MOF derived intact metal@carbon composite: An efficient cathode catalyst for aqueous and solid-state Zn-air batteries, J Energy Chem, 64 (2022) 385-394.
[31] W.G. Fang, H.B. Hu, T.T. Jiang, G. Li, M.Z. Wu, N- and S-doped porous carbon decorated with in-situ synthesized Co-Ni bimetallic sulfides particles: A cathode catalyst of rechargeable Zn-air batteries, Carbon, 146 (2019) 476-485.
[32] J.C. Li, Y. Meng, L.L. Zhang, G.Z. Li, Z.C. Shi, P.X. Hou, C. Liu, H.M. Cheng, M.H. Shao, Dual-Phasic Carbon with Co Single Atoms and Nanoparticles as a Bifunctional Oxygen Electrocatalyst for Rechargeable Zn-Air Batteries, Adv Funct Mater, 31 (2021).
[33] Q.Y. Zhou, Z. Zhang, J.J. Cai, B. Liu, Y.L. Zhang, X.F. Gong, X.L. Sui, A.P. Yu, L. Zhao, Z.B. Wang, Z.W. Chen, Template-guided synthesis of Co nanoparticles embedded in hollow nitrogen doped carbon tubes as a highly efficient catalyst for rechargeable Zn-air batteries, Nano Energy, 71 (2020).
[34] X.D. Duan, S.S. Ren, F.Y. Ge, X.K. Zhu, M.D. Zhang, H.G. Zheng, MOF-derived CoNi,CoO,NiO@N-C bifunctional oxygen electrocatalysts for liquid and all-solid-state Zn-air batteries, Nanoscale, 13 (2021) 17655-17662.
[35] H.Z. Zheng, F. Ma, H.C. Yang, X.G. Wu, R. Wang, D.L. Jia, Z.X. Wang, N.D. Lu, F. Ran, S.L. Peng, Mn, N co-doped Co nanoparticles/porous carbon as air cathode for

highly efficient rechargeable Zn-air batteries, Nano Res, 15 (2022) 1942-1948.
[36] Y. Gao, D.B. Kong, F.L. Cao, S. Teng, T. Liang, B. Luo, B. Wang, Q.H. Yang, L.J. Zhi, Synergistically tuning the graphitic degree, porosity, and the configuration of active sites for highly active bifunctional catalysts and Zn-air batteries, Nano Res, (2022).
[37] Q. Lu, H. Wu, X.R. Zheng, Y.A. Chen, A.L. Rogach, X.P. Han, Y.D. Deng, W.B. Hu, Encapsulating Cobalt Nanoparticles in Interconnected N-Doped Hollow Carbon Nanofibers with Enriched Co-N-C Moiety for Enhanced Oxygen Electrocatalysis in Zn-Air Batteries, Adv Sci, 8 (2021).
[38] C. Yingjie, G. Chong, M. Xiangyu, C. Xing, L. Guofu, S. Qiong, P. Beili, Z. Qian, F. Jianguang, Y. Liyan, D. Lifeng, Molten Salt-Assisted Carbonization and Unfolding of Fe, Co-codoped ZIF-8 to Engineer Ultrathin Graphite Flakes for Bifunctional Oxygen Electrocatalysis, J Alloy Compd, (2022).
[39] Z. Li, X. Lin, W. Xi, M. Shen, B. Gao, Y. Chen, Y. Zheng, B. Lin, Bamboo-like N,S-doped carbon nanotubes with encapsulated Co nanoparticles as high-performance electrocatalyst for liquid and flexible all-solid-state rechargeable Zn-air batteries, Appl Surf Sci, (2022).
[40] J. Zhang, B. Cui, S. Jiang, H. Liu, M. Dou, Construction of three-dimensional cobalt sulfide/multi-heteroatom co-doped porous carbon as an efficient trifunctional electrocatalyst, Nanoscale, (2022).
[41] J. Liu, J. Zhou, M.K.H. Leung, Valence Engineering of Polyvalent Cobalt Encapsulated in a Carbon Nanofiber as an Efficient Trifunctional Electrocatalyst for the Zn–Air Battery and Overall Water Splitting, Acs Appl Mater Inter, (2022).
[42] H. Zhang, X. Wang, Z. Li, C. Zhang, S. Liu, In situ encapsulation engineering boosts the electrochemical performance of highly graphitized N-doped porous carbon-based copper–cobalt selenides for bifunctional oxygen electrocatalysis, Nanoscale, (2021).
[43] X. Zhou, X.Y. Leng, C. Ling, H.B. Chong, A.W. Xu, Z.K. Yang, Integrating a metal framework with Co-confined carbon nanotubes as trifunctional electrocatalysts to boost electron and mass transfer approaching practical applications, Nanoscale, 13

(2021) 12651-12658.